Scheme I

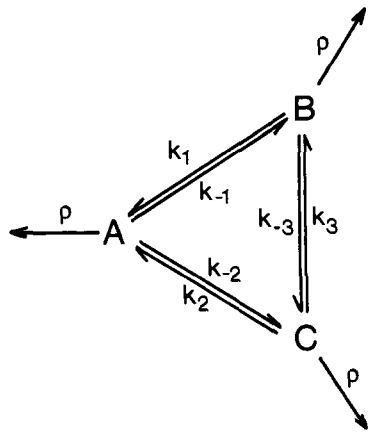

The time dependence of the exchange cross peaks and corresponding diagonal resonances in a series of NOESY spectra recorded with mixing times ranging from 10 to 300 ms at pH 5.8 is shown in Figure 2, together with the best-fit theoretical curves using the simple three-species model of Scheme I. A is the major species, B and C are the two minor species, k_i are the rate constants for interconversion between the species, and ρ is the total spin-lattice relaxation rate of the relevant proton, which for simplicity is assumed to be the same for the two histidines of all three species. The time development of magnetization in such a system is described by[5]

$$dM_A/dt = -M_A(\rho + k_{-1} + k_{-2}) + M_B k_1 + M_C k_2$$
$$dM_B/dt = -M_B(\rho + k_1 + k_{-3}) + M_A k_{-1} + M_C k_3 \quad (1)$$
$$dM_C/dt = -M_C(\rho + k_2 + k_3) + M_A k_{-2} + M_B k_{-3}$$

The equilibrium constants between the species are defined as $K_1 = k_1/k_{-1} = [A]/[B]$, $K_2 = k_2/k_{-2} = [A]/[C]$, and $K_3 = k_3/k_{-3} = [B]/[C] = K_2/K_1$. The intensity of a given diagonal peak and its associated cross peaks as a function of mixing time t is obtained by solving eq 1 with the magnetization of the species corresponding to the diagonal peak set to 1 in the case of the major species A (and to $1/K_1$ or $1/K_2$ in the case of minor species B or C) and the magnetization of all other species set to 0. The complete set of build-up curves was fitted *simultaneously* by carrying out successive numerical integration runs under control of a nonlinear least-squares optimization routine, varying the values of the rate constants k_1, k_{-1}, k_2, k_{-2}, and ρ, and a scale factor. The exact values of k_3 and k_{-3} have a minimal effect on the system as the equilibrium constant K_3 is determined by the other two equilibrium constants, so that for simplicity k_{-3} was set to 10^{-4} s^{-1}.

The diagonal and exchange cross peaks of the two histidine residues exhibit the same time dependence, indicating that they are associated with the same dynamical processes. The results of the analysis are summarized in Table I for data collected at pH 5.8 and 7.0. At pH 5.8, 91.3% of the zinc finger is in form A, 5.3% in form B, and 3.4% in form C, and there is no significant change in these values at pH 7.0. The main difference between the data at pH 5.8 and 7.0 lies in the rates for the interconversion between species A and C, which are approximately half those at pH 5.8.

At pH values above 5.5 the equilibrium constant for the binding of zinc to the peptide is $\geq 10^6$ M^{-1} so that, under the experimental conditions employed, the concentration of zinc-free peptide is $\ll$0.01% of the total peptide present. Thus, the simplest explanation for the observed exchange phenomena is one in which both histidines are liganded to zinc in species A, while in species B and C, only one of the histidine residues is liganded to the metal with the fourth coordination position either unoccupied or possibly taken by a water molecule. Examination of the structure of the zinc finger[1] indicates that only a small change in the χ_2 angle of the histidines is required to accomplish this. The downfield shift of the histidine resonances of the two minor forms can probably be attributed to a partial net positive charge on the zinc atom arising from the change in histidine coordination and resulting in deshielding of the histidine imidazole protons.

Table I. Equilibrium and Rate Constants for Scheme I Obtained from a Nonlinear-Least-Squares Fit to the Experimental Data at 6 °C

	pH 5.8	pH 7.0
k_1 (s^{-1})	7.8 ± 1.1	6.7 ± 0.5
k_{-1} (s^{-1})	0.5 ± 0.03	0.4 ± 0.03
k_2 (s^{-1})	16.3 ± 1.8	8.8 ± 0.8
k_{-2} (s^{-1})	0.6 ± 0.05	0.4 ± 0.05
K_1	17.1 ± 1.5	17.2 ± 1.1
K_2	28.5 ± 1.4	24.0 ± 1.5
K_3	1.7 ± 0.1	1.4 ± 0.1
ρ (s^{-1})	2.9 ± 0.2	2.6 ± 0.4

The present data clearly indicate the presence of dynamical transitions between a major and two minor species of a zinc finger domain which occur on time scales in the millisecond to second range. Although the occupancy of these minor species is low, namely, of the order of a few percent, they are nevertheless easily observable, and any naive interpretation of the associated cross peaks may have led to incorrect conclusions.

Note Added in Proof. Two recent reports on zinc finger peptides (Kochoyan et al. *Biochemistry* **1991**, *30*, 3371; Xu et al. *Ibid.* **1991**, *30*, 3365) suggest the possibility of multiple conformations although no proof as exemplified by exchange cross peaks was presented.

Acknowledgment. We thank Drs. E. Appella and K. Sakaguchi for useful discussions. This work was supported by the AIDS Directed Anti-Viral Program of the Office of the Director of the National Institutes of Health (G.M.C. and A.M.G.).

Ab Initio Studies of a Marginally Stable Intermediate in the Base-Catalyzed Methanolysis of Dimethyl Phosphate and Nonexistence of the Stereoelectronically Unfavorable Transition State

Tadafumi Uchimaru,*[†] Kazutoshi Tanabe,[†] Satoshi Nishikawa,[‡] and Kazunari Taira*[‡]

National Chemical Laboratory for Industry and Fermentation Research Institute Agency of Industrial Science & Technology MITI, Tsukuba Science City 305, Japan

Received October 16, 1990

A pentacoordinated oxyphosphorane, whose properties are not easily elucidated experimentally, is a common intermediate/transition state for the hydrolysis and transesterification of phosphate esters. RNA cleaving reactions proceed via a five-membered cyclic oxyphosphorane.[1-3] Previously, we carried out ab initio STO-3G studies on cyclic oxyphosphorane dianion **2a** as a model compound for the RNA cleaving process (**1**).[4] The calculations indicated that the transition state for the exocyclic P–O_5 bond breaking step is higher in energy than that for the endocyclic P–O_2 bond breaking step (rapid equilibrium). The origin of the energy difference between these two transition states is likely to be attributable to a combination of stereoelectronic

[†] National Chemical Laboratory for Industry.
[‡] Fermentation Research Institute.

(1) Breslow, R.; Labelle, M. *J. Am. Chem. Soc.* **1986**, *108*, 2655-2659.
(2) Anslyn, E.; Breslow, R. *J. Am. Chem. Soc.* **1989**, *111*, 4473-4482.
(3) Taira, K. *Bull. Chem. Soc. Jpn.* **1987**, *60*, 1903-1909.
(4) Taira, K.; Uebayasi, M.; Maeda, H.; Furukawa, K. *Protein Eng.* **1990**, *3*, 691-701.

0002-7863/91/1513-4351$02.50/0

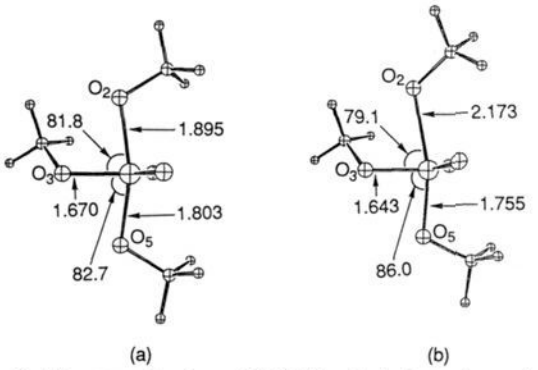

Figure 1. The ORTEP drawings of 3-21G* optimized structures of pentacoordinated oxyphosphorane **3a**: (a) the stable pentacoordinated intermediate; (b) the transition state for the P–O_2 bond translating step. The structural parameters are given in angstroms and degrees. The total energies (au) of the intermediate and the transition state are −829.450 12 and −829.447 97, respectively. The imaginary frequency computed for the transition structure is 152.8*i* cm^{-1}.

effects[5] and ring strain. Recently, Lim and Karplus reported ab initio calculations on a similar compound **2b**.[6] In their studies with higher basis sets, in contrast to our STO-3G calculations, no dianionic pentacoordinated intermediate was located. In order to eliminate the effects of the ring strain and to examine the magnitude of the stereoelectronic effects, we have now characterized dianionic trimethoxyphosphorane **3a**, the acyclic counterpart of **2a**. In the present communication, we report 3-21G* calculations that show that, in contrast to **2b**,[6] the dianionic species **3a** *does exist* as a marginally stable intermediate having a distorted trigonal bipyramidal structure.

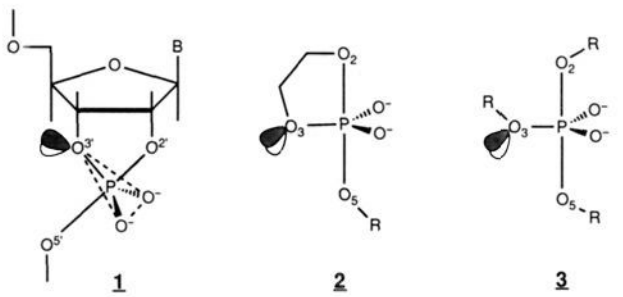

a: R = Me
b: R = H

According to the theory of stereoelectronic effects, antiperiplanar lone pairs may assist both nucleophilic attack and axial group displacement in this system. Equatorial P–O_3 bond rotation during the reaction provides the mechanism for a stereoelectronic assist in both reaction steps.[7] We report on the ab initio reaction profile for the base-catalyzed methanolysis of dimethyl phosphate monoanion, including such bond rotational processes, which clearly show that rotation about the equatorial P–O_3 bond during the reaction is required for the lowest energy pathway.[8]

In **3a**, the antiperiplanar lone pairs on O_3 are available only to the P–O_2 bond, and not to the P–O_5 bond (see the optimized structures in Figure 1). Accordingly, the P–O_2 bond cleavage in **3a** is considered to be stereoelectronically facilitated, while the

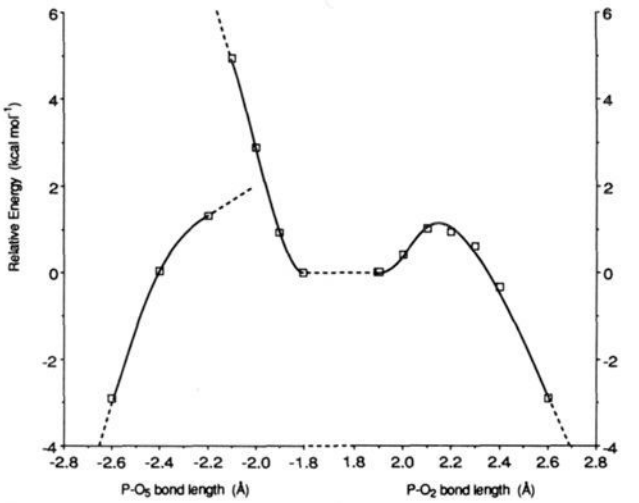

Figure 2. The 3-21G* reaction profile for the P–O_2 and P–O_5 axial bond cleavages from the trigonal-bipyramidal pentacoordinated oxyphosphorane **3a**. The vertical axis shows the relative energy with respect to the stable intermediate, whose structure is shown in Figure 1a.

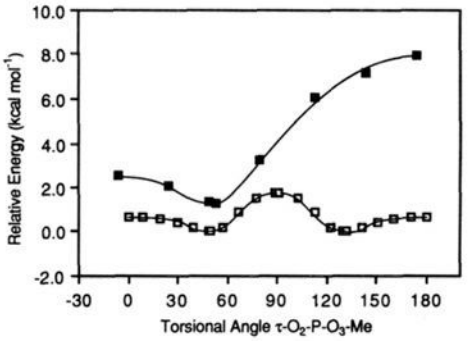

Figure 3. The energy profiles for the rotation of the equatorial P–O_3 bond in oxyphosphorane **3a**. The vertical axis represents the relative energy with respect to the stable intermediate. The solid line connecting open squares represents the rotational energy profile in the metastable state (bottom). Complete geometry optimization was carried out for each rotamer. The closed squares show the rotation energy profile in the P–O_2 translating step (top). The translating P–O_2 bond length was fixed at the value of the transition state, and the other structural parameters were optimized at each torsional angle. The ORTEP drawings shown in parts a and b of Figure 1 correspond to the structures at the minimum points of the profiles.

P–O_5 bond cleavage in **3a** is unfavorable.[5] The 3-21G* reaction profile is shown in Figure 2.[9] The transition state for the P–O_2 bond breaking step with only one imaginary frequency of 152.8*i* cm^{-1} was located. The motion of atoms in the normal modes corresponding to the imaginary frequency is in the direction connecting the oxyphosphorane **3a** and the reactants (methoxide anion and dimethyl phosphate monoanion). Characteristic of an early transition state, the fully optimized structure of the P–O_2 bond breaking transition state is not far from the intermediate structure, as shown in parts a and b of Figure 1.

In contrast to the stereoelectronically favorable P–O_2 bond breaking, the transition state for the stereoelectronically unfavorable P–O_5 bond breaking step could not be located. At an increased P–O_5 bond length of 2.2 Å, equatorial P–O_3 bond rotation occurred and resulted in a structure with the equatorial methoxyl group occupying the same side of the breaking P–O_5

(5) Gorenstein, D. G. *Chem. Rev.* **1987**, *87*, 1047–1077. Deslongchamps, P. *Stereoelectronic Effects in Organic Chemistry*; Pergamon Press Ltd.: New York, 1983. Kirby, A. J. *The Anomeric Effects and Related Stereoelectronic Effects at Oxygen*; Springer-Verlag: Berlin, 1983.

(6) Lim, C.; Karplus, M. *J. Am. Chem. Soc.* **1990**, *112*, 5872–5873.

(7) Gorenstein, D. G.; Luxon, B. A.; Findlay, J. B. *J. Am. Chem. Soc.* **1979**, *101*, 5869–5875.

(8) In the present study, ab initio calculations were carried out at the RHF/3-21G* level on trigonal-bipyramidal trimethoxyphosphorane dianion **3a**. All the calculations were carried out by using the GAUSSIAN 86 program (Carnegie-Mellon Quantum Chemistry Publishing Unit, Pittsburgh, PA, 1984) on FACOM M780/MSP and IBM 3090/MVS computers.

(9) The reaction profile for the base-catalyzed methanolysis of dimethyl phosphate was explored starting from the geometry of the stable intermediate **3a** (Figure 1a). The distances between methoxyl $O_{2,5}$ and P were employed as the reaction coordinates for methoxyl group attack and displacement steps. The points comprising the reaction profile were obtained through the geometry optimization at each value of the reaction coordinate without any additional constraint.

bond, depicted in the −2.6 to −2.2 Å region of Figure 2 (negative sign merely represents P–O_5 translation). The resulting structure is very similar, by symmetry, to the stereoelectronically favored P–O_2 transition state geometry shown in Figure 1b.

We next explored the energy profile for the rotation of the equatorial P–O_3 bond in oxyphosphorane **3a** to examine the stereoelectronic effects in the intermediate and the transition state. In Figure 3, the rotational profile (top) for the axial P–O_2 bond breaking step is plotted with the rotational profile (bottom) of the metastable intermediate **3a**.[8,10] The rotational energy profile for the axial P–O_2 bond breaking step was calculated with the fixed P–O_2 bond length of 2.173 Å, which is the calculated value at the P–O_2 bond breaking transition state (Figure 1b). In the rotational energy profile for the P–O_2 bond breaking step, one of the two metastable-state local minima at a $\tau(O_2PO_3Me)$ of around 130°, corresponding to the stereoelectronically unfavorable P–O bond breaking pathway, has completely disappeared. This is in accord with P–O_3 bond rotation at the increased P–O_5 bond length of 2.2 Å (see Figure 2).

The energy profiles shown in Figures 2 and 3 indicate that a stereoelectronically unfavorable transition state with only one negative eigenvalue should be unattainable: Even though the energy increases with P–O_5 bond lengthening in the −2.0 to −2.2 Å region (Figure 2), the energy well at a $\tau(O_2PO_3Me)$ of around 130° has already disappeared when the P–O_2 bond length is 2.173 Å (Figure 3).[11-13] It is also noteworthy that the metastable-state stereoelectronic effect is ca. 2 kcal mol^{-1} as evidenced from the bottom profile connecting open squares in Figure 3; on the other hand, the stereoelectronic effect at the transition state is at least 6 kcal mol^{-1} as extrapolated at the point of $\tau(O_2PO_3Me)$ = 130° and P–O_5 = 2.173 Å of the top profile. In reality, a transition-state stereoelectronic effect must be much larger than 6 kcal mol^{-1}, because the putative transition state for the P–O_5 bond cleavage step would be expected to occur much later at P–O_5 > 2.7 Å if the stereoelectronically unfavorable transition state could have existed as in **2a**. In fact, under C_s symmetry, the energy difference between the stereoelectronically favorable and unfavorable transition states in **3b** was calculated to be ca. 29 kcal mol^{-1} [12] These results support earlier emphasis that the kinetic stereoelectronic effect and the α-effect are largely transition-state phenomena.[14]

Since the present results suggest that the stereoelectronically[15] unfavored axial P–O bond cleavage and formation should not occur in the acyclic oxyphosphorane system, the equatorial P–O_3 bond rotation during the reaction must be essential for the axial attack and axial departure (in-line) mechanisms in the base-catalyzed acyclic phosphate ester methanolysis. The relative energies of the transition states for the axial P–O bond cleavage and for the equatorial P–O bond rotation are calculated to be comparable, and both have activation energies of less than 2 kcal mol^{-1} with respect to the metastable intermediate **3a**.[16] Thus, all events consisting of attack, rotation, and cleavage after rotation turn out to be only partially rate determining.[17]

The recent report by Lim and Karplus[6] suggesting the nonexistence of the dianionic intermediate of cyclic oxyphosphorane system **2b** is in contrast to the acyclic oxyphosphorane system **3a** presented here. The cause for this discrepancy does not seem to arise from the cyclic nature of **2b**, since our calculations at the 3-21G* level of theory also support the existence of the dianionic intermediate **2a**.[13] Instead, the contrast can be reconciled by the difference of the axial substituents (OH vs OMe). Bigger substituents probably better delocalize the dianionic charges and stabilize the intermediates in the gas phase.[18] Consequently, in the case of Karplus's system, less stable **2b** abolished the stereoelectronically favorable P–O_2 bond breaking transition state, leaving only the P–O_5 bond breaking transition state.

(10) The rotational energy profiles for the metastable state and for the P–O_2 bond breaking step were explored starting from the local-minimum geometry of the metastable state (Figure 1a) and from the P–O_2 transition-state geometry (Figure 1b). Each point comprising the energy profiles was obtained by the geometry optimization at each torsional angle.

(11) A P–O_5 transition state for **3b** with the P–O_5 bond length of 3 Å was found at 3-21G* level under C_s symmetry restricted conditions,[12] corresponding to unfavorable P–O_5 bond breaking in this study. Moreover, because of the unique cyclic nature of **2a**, its 3-21G* transition state for stereoelectronically unfavorable exocyclic P–O_5 bond cleavage has been located, without assuming any symmetry, at the P–O_5 bond length of 2.728 Å.[19] Note that, in terms of the orientation of lone-pair electrons on O_3, the P–O_5 bond in **2a** is equilivalent to the P–O_5 bond in **3a**. Our results presented here indicate that the stereoelectronically unfavorable transition state occurring with such a long bond distance should not be possible in the acyclic system.

(12) Taira, K.; Uchimaru, T.; Tanabe, K.; Uebayasi, M.; Nishikawa, S.; *Nucleic Acids Res.*, in press.

(13) Storer, J. W.; Uchimaru, T.; Tanabe, K.; Uebayasi, M.; Nishikawa, S.; Taira, K. *J. Am. Chem. Soc.*, in press.

(14) Taira, K.; Gorenstein, D. G. *J. Am. Chem. Soc.* **1984**, *106*, 7825-7831.

(15) Note that the energy profiles in Figure 3 can be explained by the optimal orbital interactions between nonbonding lone pair orbitals on equatorial oxygen and antibonding σ* orbitals of axial P–O bonds.[5] We call this reactivity dependence on the orientation of lone-pair electrons a "stereoelectronic effect", although we do not know the exact origin of the effect as to whether it is due to orbital mixing or other factors, since the overlap populations and Mulliken charges calculated for oxyphosphorane species **3a** are not necessarily in accord with the orbital mixing interpretation.

(16) The energy well around the metastable intermediate **3a** remains after zero point energy correction at the three stationary points optimized at the 3-21G* level: the metastable intermediate and the transition state for the axial P–O bond breaking and for the equatorial P–O bond rotation. The well depth is calculated to be 0.54 kcal mol^{-1} at the 3-21G* level with zero-point energy included.

(17) Consequently, for the lowest energy pathway of methoxide attack on dimethyl phosphate monoanion: (i) MeO^- attacks phosphorus following the right half profile of Figure 2 (P–O_2 bond length of 2.8–1.9 Å region); (ii) the equatorial MeO group rotates following the bottom profile of Figure 3 (from a $\tau(O_2PO_3Me)$ value of 50.1° to 129.9°, corresponding to two local minima of the metastable state); and (iii) MeO^- leaves following the reversed pathway of (i) because of the structural symmetry.

(18) Under C_1 symmetry, the oxyphosphorane species **3b** does not exist as a stable intermediate.[12] However, recent work by Karplus et al. shows that, for the attack of OH^- on dimethyl phosphate monoanion, an intermediate does exist at the 3-21G* and 3-21+G* level, and they obtained an energy profile like Figure 2 of this study.[20] Moreover, our unpublished results on *monoanionic* **2a** indicate that it is a much more stable intermediate than *dianionic* **2a**. These results are in accord with our interpretation of delocalized charges. Furthermore, solvation should stabilize a dianionic intermediate relative to two monoanionic reactants (see also the conclusion of ref 13).

(19) Taira, K.; Uchimaru, T.; Storer, J. W.; Tanabe, K.; Nishikawa, S., manuscript in preparation.

(20) Dejaegere, A.; Lim, C.; Karplus, M. *J. Am. Chem. Soc.*, following paper in this issue.

Dianionic Pentacoordinate Species in the Base-Catalyzed Hydrolysis of Ethylene and Dimethyl Phosphate†

A. Dejaegere,‡ C. Lim,§ and M. Karplus*

Department of Chemistry, Harvard University
Cambridge, Massachusetts 02138

Received February 4, 1991

The nature of the pentacoordinate species involved in the hydrolysis of phosphate esters in enzymes and aqueous solution is still unclear. Recently, we reported gas phase ab initio calculations[1] which showed that there is no dianionic pentacoordinate intermediate along the gas-phase reaction path for the basic hydrolysis of ethylene phosphate, a model for the rate-determining step in the enzymatic hydrolysis of RNA by bovine ribonuclease A.[2] Specifically, in the nucleophilic attack by OH^- on the cyclic ester, ethylene phosphate (i.e., $OH^- + (CH_2O)_2PO_2^- \rightarrow HOCH_2CH_2OPO_3^{2-}$), a pentacoordinate dianionic species is a transition state but not an intermediate at the Hartree–Fock 3-21G* or 3-21+G* ab initio level,[3] even though STO-3G cal-

†Supported in part by a grant from the National Science Foundation.
‡Supported by the Belgian National Fund for Scientific Research.
§Present address: Department of Medical Genetics, Medical Science Building, University of Toronto, Toronto, Ontario, M5S 1A8 Canada.

(1) Lim, C.; Karplus, M. *J. Am. Chem. Soc.* **1990**, *112*, 5872.

(2) Fersht, A. *Enzyme Structure and Mechanism*; W. H. Freeman & Co.: New York, 1985.

0002-7863/91/1513-4353$02.50/0